Enhancement of electrochemical and photoelectrochemical properties of fibrous Zn and ZnO electrodes†

Carmen M. López and Kyoung-Shin Choi*

Zinc and zinc oxide electrodes with fibrous morphologies were prepared to exploit their high interfacial areas and superior electrical conductivity for the enhancement of electrochemical and photoelectrochemical properties.

Zinc and zinc oxide are main components of a variety of electrodes used in batteries, zinc–air cells, photovoltaics, and CO_2 reduction.[1] The abundance and nontoxicity of zinc makes development of zinc-based devices attractive and practical. The selectivity, reversibility, and reactivity of the electrodes used in these applications rely on the chemical and physical factors that define the energetics and kinetics at the electrodes' interface.[2] These factors, in turn, are significantly affected by morphological features at the interfaces (*e.g.* size, shape, grain boundary, interconnection of the particles). Therefore, controlling macro-, micro-, and nano-structural features at the interfaces and understanding their effects on desired chemical and electrochemical properties are the key to producing high performance, low cost, and lightweight electrode materials.

Production of electrode materials with fibrous morphology has been of special interest because it not only increases the surface area, but also provides superior electrical conductivity when compared to other morphologies of equal surface areas.[3] The intrinsic porous features created by fibrous morphology can also substantially alleviate swelling and deformation problems caused by oxidation–reduction cyclings of rechargeable batteries.[4] To date, many inorganic materials have been prepared with rod, belt, and wire shapes.[5] However, growing fibers/wires from a conducting substrate with good electrical contact for use as electrodes materials has been extremely rare. This has limited the opportunity to characterize and exploit fibrous electrodes for efficient, cost-effective, and lightweight devices. In this study, we describe the electrochemical synthesis of fibrous zinc electrodes, which can be thermally oxidized to zinc oxide electrodes while preserving the original fibrous morphology. Preliminary electrochemical and photoelectrochemical properties of the resulting electrodes were investigated to probe the possibility of utilizing them for zinc–air cells and photoelectrochemical cells.

Zinc films were electrochemically deposited from dimethyl sulfoxide (DMSO) solutions containing 0.03 M $Zn(ClO_4)_2 \cdot 6H_2O$ as the zinc source and 0.1 M $LiClO_4 \cdot 3H_2O$ as the supporting electrolyte.[6] DMSO was chosen as a plating medium because it offers a wider range of deposition temperatures (*i.e.* boiling point of DMSO, 189 °C) and deposition potentials than aqueous solutions.[7] This creates more synthetic freedom to regulate the

morphologies of inorganic deposits by formulating deposition conditions.

Among the range of potentials investigated (-0.8 V $\leqslant E \leqslant -3.0$ V), -1.5 V was optimum for systematically studying the effect of temperature on morphology changes of Zn films. Potentials more positive than -1.4 V resulted in significant co-deposition of ZnO while potentials more negative than -1.54 V caused poor adhesion of the Zn films to the substrate at temperatures above 100 °C.

Fig. 1 shows scanning electron micrographs of Zn films deposited on Ti substrates with temperatures ranging from 60–125 °C at $E = -1.5$ V. At lower temperatures the morphology of the deposited films is characterized by compactly packed round particles (Fig. 1a). As the temperature increases, the current density and therefore the deposition rate increases gradually (*e.g.* 1.4 mA cm^{-2}, 2.0 mA cm^{-2}, 4.4 mA cm^{-2}, and 6.5 mA cm^{-2} for 60 °C, 70 °C, 90 °C, and 125 °C, respectively), and the zinc deposits begin to develop the interconnectivity characteristic of fibers. The individual particulate features can still be distinguished in the films deposited at temperatures below 110 °C (Fig. 1b–c), while fibrous character becomes dominant for films deposited above 110 °C. The most uniform growth of fibrous zinc film can be obtained at temperatures of 125 $\pm$ 2 °C (Fig. 1d). This fibrous growth can be
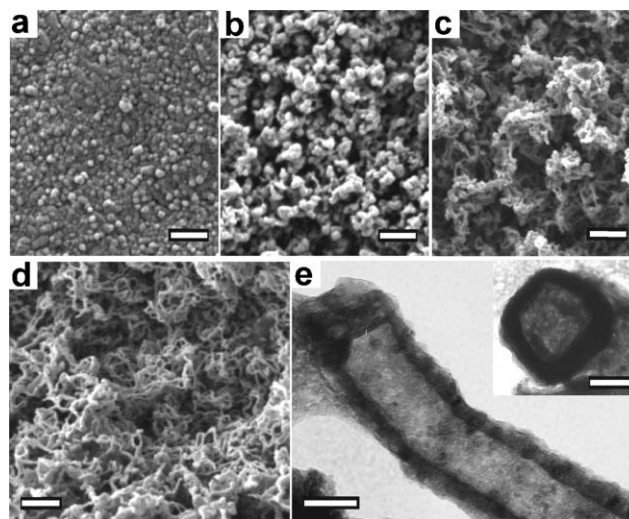

Fig. 1 SEM images of Zn films deposited at (a) 60 °C, (b) 70 °C, (c) 90 °C, and (d) 125 °C. (d) TEM image of an individual fiber. The inset shows the tip of the fiber (Scale bar: (a)–(d); 1 μm, (e); 50 nm). All the films shown here and used for further characterization were deposited by passing a fixed amount of total charges (3.003 C) through the working electrode so that each electrode possesses the same amount of Zn deposits.

---

considered a type of dendritic growth, which can be initiated when the deposition rate exceeds the diffusion rate of the Zn^{2+} ions, creating diffusion limited conditions.[8]

Transmission electron microscopy (TEM) revealed that these fibers are tubular with hollow cores, which is unambiguously determined by a lighter central region and darker edges of the fiber, as well as the opening of the fiber shown in Fig. 1e. The walls of the fibers are polycrystalline and are composed of roughly spherical particles with an average diameter of 6–10 nm.

Zn electrodes with fibrous morphology have been predicted to be the optimum anodes for use in electrically rechargeable zinc–air cells.[3] Compared to conventional zinc electrodes that utilize micron size zinc powder connected with binding materials, a fibrous electrode may achieve good electrical continuity with no need for binding materials. In addition, its enhanced surface area may significantly increase the current density, and therefore the power density of the cell. Fig. 2 shows cyclic voltammograms (CV) of the fibrous zinc electrodes, along with the Zn electrode deposited at 60 °C and a zinc foil of the same geometrical area (1.73 cm^2), which provides a direct comparison of their electrochemical activities.

The recorded voltammograms show good agreement with those of zinc electrodes reported in the literature.[9] The anodic peak A1 corresponds to the oxidation of Zn^0 to the soluble zincate ion $Zn(OH)_4^{2-}$, and peak A2 corresponds to $Zn(OH)_3^-$ that forms due to depletion of OH^- in solution near the electrode surface. The cathodic peak C1 is attributed to the reduction of Zn^{2+} to Zn^0. The current densities observed at the cathodic peak (or anodic peaks) increase as the porosity and interfacial areas of the films increase. Judging from the total charges integrated under the cathodic peak, the electrochemically active interfacial areas of the fibrous film (75.1 mC) is approximately 8 times larger than that of zinc foil (9.5 mC). This observation proves that due to the good connectivity of the particles forming the fibrous morphology, any possible disadvantages of having high surface areas (e.g. boundary scattering, electrical isolation) can be minimized, resulting in a substantially enhanced overall performance of fibrous electrodes. These results encourage further investigation to probe the possibility of assembling an electrically rechargeable zinc–air cell using the as-deposited fibrous zinc electrode. It should also be noted that the distance between the cathodic and anodic peaks in the CV of the fibrous electrode increases as the interfacial areas increase. This indicates extremely slow electron transfer kinetics
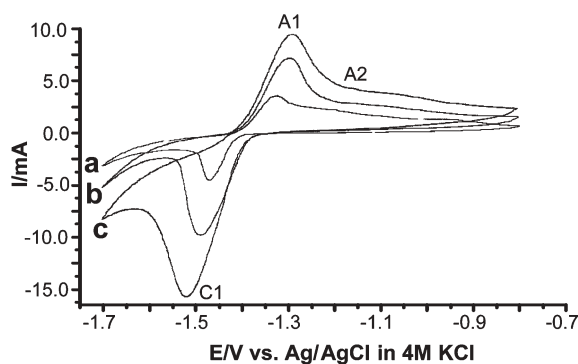
involved in Zn/Zn^{2+} redox reactions occurring at the electrode surface.[9]

The fibrous morphology may also be beneficial for semiconducting ZnO electrodes for use in dye sensitized solar cells and photoelectrochemical cells, because the efficiency of these devices is critically affected by the interfacial areas and electrical continuity of the electrodes used.[10] Fibrous ZnO electrodes cannot be directly obtained electrochemically because the current density required to generate the fibrous morphology cannot be obtained by potentials that allow the deposition of pure ZnO. However, they can be prepared by heating the fibrous Zn electrodes at 450 °C for 90 minutes, the mildest conditions that completely oxidize Zn to ZnO. The purity of the ZnO electrodes after thermal oxidation was confirmed by X-ray diffraction (XRD) (Fig. 3(a)). The trace of ZnO appearing in the XRD pattern of as-deposited Zn film is due to surface oxidation. The SEM and TEM studies of the ZnO film show that most of the original fibrous and tubular features remain intact with minor aggregation phenomena (Fig. 3(b)–(c)). The other Zn electrodes shown in Fig. 1(a)–(c) were also thermally converted to ZnO electrodes for further characterization, preserving their morphologies under identical heating conditions.

The photoelectrochemical properties of the resulting ZnO electrodes were characterized by measuring the photocurrent at zero-bias, which is a direct, quantitative measure of redox activity generated by light. Because these electrodes are prepared and treated in nearly identical conditions, changes in their photoelectrochemical properties can be solely ascribed to the variation of their morphological features. All ZnO electrodes generate anodic photocurrents due to their n-type character; oxygen is produced at the semiconductor–electrolyte interface by using photogenerated holes, while the photogenerated electrons are transferred to the Pt counter electrode through the external circuit to generate hydrogen.[10] Plots shown in Fig. 4 clearly demonstrate a systematic trend of increasing photocurrent as the surface area of the ZnO
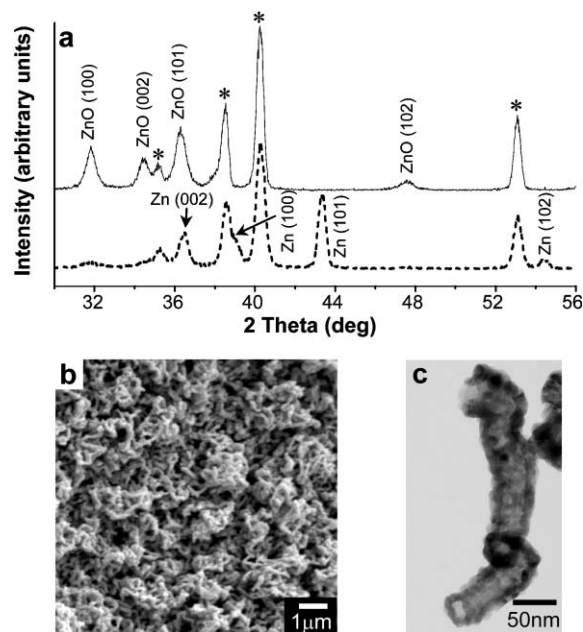

Fig. 3 (a) XRD patterns of fibrous electrodes before (---) and after (—) thermal oxidation (* indicates peaks generated by Ti substrates). (b) SEM and (c) TEM images of fibrous ZnO films.
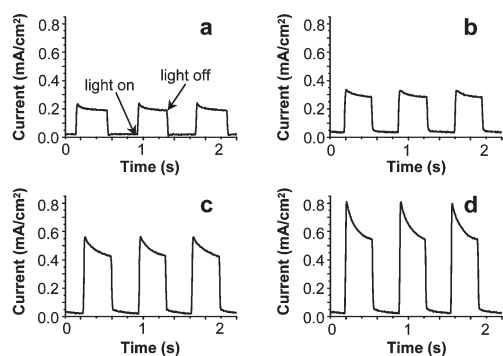

Fig. 2 CVs of (a) zinc foil and Zn films deposited at (b) 60 °C and (c) 125 °C, measured in 0.2 M KOH$_{(aq)}$ solution (scan rate: 17 mV s^{-1}).

Fig. 4 Photocurrent measured at zero-bias for ZnO films prepared from Zn electrodes deposited at (a) 60 °C, (b) 70° C, (c) 90 °C, and (d) at 125 °C. A 0.1 M aqueous KNO$_3$ solution was used as electrolyte. Illumination was provided by a chopped Xe light source (300 W) and the incident light flux was 4.66 W cm^{-2}.

electrodes increase. The fibrous ZnO electrode (Fig. 4(d)) exhibits 3 times higher photocurrent than the ZnO electrode converted from Zn electrode deposited at 60 °C (Fig. 4(a)). The ZnO electrode obtained by thermally oxidizing zinc foil with a flat surface does not generate any detectable photocurrent at zero-bias due to its low surface area. These results clearly demonstrate that even without varying the compositions of materials, photocurrent can be considerably improved by optimizing morphological features. The fibrous ZnO electrodes are expected to serve as excellent host electrodes to further assemble multi-component photoelectrodes (*i.e.* dye sensitized solar cells, heterojunction photoelectrodes).

In summary, practical and facile routes for the preparation of fibrous Zn and ZnO electrodes have been developed. By characterizing the electrochemical and photoelectrochemical properties of Zn and ZnO electrodes with systematically varying surface morphologies, this study demonstrates the superiority of fibrous morphology and, more importantly, the significance of interfacial engineering for maximizing desired functional properties. Extreme deposition conditions achieved by exploiting non-aqueous plating media (*i.e.* high deposition potentials and temperatures) may be capable of producing a broader range of electrode materials with the desired fibrous morphology.

Carmen M. López and Kyoung-Shin Choi*
Department of Chemistry, Purdue University, West Lafayette, IN 47907, USA. E-mail: kchoi1@purdue.edu; Fax: 765-494-0239; Tel: 765-494-0049

Notes and references

1 F. Beck and P. Rüetschi, *Electrochim. Acta*, 2000, **45**, 2467; B. O'Regan, D. T. Schwartz, S. M. Zakeeruddin and M. Grätzel, *Adv. Mater.*, 2000, **12**, 1263; J. Goldstein, I. Brown and B. Koretz, *J. Power Sources*, 1999, **80**, 171; K. Ohta, M. Kawamoto and T. Mizuno, *J. Appl. Electrochem.*, 1998, **28**, 717.

2 A. Katoh, H. Uchida, M. Shibata and M. Watanabe, *J. Electrochem. Soc.*, 1994, **141**, 2054.

3 L.-F. Li, M. G. Stevens, T. Tsai and R. Lemieux, *International Patent*, 2002, No. WO02/069422 A2.

4 J.-M. Tarascon and M. Armand, *Nature*, 2001, **414**, 359.

5 Z. L. Wang, *Annu. Rev. Phys. Chem.*, 2004, **55**, 159; C. N. R. Rao, F. L. Deepak, G. Gundiah and A. Govindaraj, *Prog. Solid State Chem.*, 2003, **31**, 5.

6 A conventional three-electrode set-up in an undivided cell was used. Titanium foil and an Ag/AgCl electrode in 4 M KCl solution were used as working and reference electrodes. For the counter electrode, 100 Å of titanium followed by 500 Å of platinum were deposited on clean glass slides by sputter coating.

7 D. Aurbach and I. Weissman, in *Nonaqueous Electrochemistry*, ed. D. Aurbach, Marcel Dekker, New York, 1999, p. 1.

8 F. Sagués, M. Queralt López-Salvans and J. Claret, *Phys. Rep.*, 2000, **337**, 97; I. Das, S. S. Mishra, N. R. Agrawal and K. S. Gupta, *J. Indian Chem. Soc.*, 2003, **80**, 351.

9 H.-J. Park and S.-I. Mho, *Anal. Sci.*, 1997, **13**, 311; M. Cai and S.-M. Park, *J. Electrochem. Soc.*, 1996, **143**, 2125.

10 M. Grätzel, *Nature*, 2001, **414**, 338.